Inorg. Chem. **2007**, *46*, 10221–10228

Magneto–Structural Correlation in a Series of Bimetallic Alternating Chain Complexes of $[Cr^{III}L(CN)_4]_n[Mn^{III}(salpn)]_n \cdot n$Solvents (L = 2,2′-bipy or 9,10-phen, salpn = Substituted Salicyldehyde, Solvents = Water and Methanol)

Feng Pan, Zhe-Ming Wang, and Song Gao*

Beijing National Laboratory for Molecular Sciences, State Key Lab of Rare Earth Materials Chemistry and Applications, College of Chemistry and Molecular Engineering, Peking University, Beijing 100871, People's Republic of China

Received July 12, 2007

Five chain compounds based on the building block of $[Cr(L)(CN)_4]^-$ (L = 2,2′-bipy, **1**–**4**; L = 9,10-phen, **5**) and $[Mn(salpn)]^+$ (salpn = substituted salicyldehyde-type Schiff base in Scheme 1) have been prepared and characterized structurally and magnetically. The four compounds (**1**–**4**) consisting of $[Cr(bipy)(CN)_4]^-$ units possess straight bimetallic chains as the $[Cr(bpy)(CN)_4]^-$ unit links the two neighbor $[Mn(salpn)]^+$ units with the two *trans*-cyanide ligands, while in **5** the chain is zigzag because the $[Cr(phen)(CN)_4]^-$ unit connects the $[Mn(salpn)]^+$ units with its two *cis*-cyanide ligands. The bond angles of Mn–N–C–Cr are adjusted by different coligands of salpn and bipy/phen. The chains are stacking via mainly the aromatic π–π-type interactions. All compounds show 3D antiferromagnetic ordering with Néel temperatures ranging from 3.7 to 8.1 K, and they are metamagnets displaying antiferromagnetic to ferrimagnetic transition at critical fields of 4.0–13.1 kOe at 1.9 K. This is due to weak interchain antiferromagnetic interactions between the ferrimagnetic bimetallic chains in the materials. The intrachain couplings (J, in cm^{-1}) in the materials, between cyanide-bridged Cr^{III} and Mn^{III} ions, from –1.84 to –5.35 cm^{-1}, follow a linear relationship ($J = -33 + 0.18\alpha$) to the Mn–N–C angles (α, in deg). In addition, the weak interchain antiferromagnetic interactions and critical fields for antiferromagnetic–ferrimagnetic transition are closely related to some of their structural factors, which were studied very superficially only referring to the separations of nearest chains in each material.

Introduction

Study of cyanide-bridged metal complexes is an old but evergreen branch in molecular magnetism. A large number of cyanide-bridged compounds, which are well known, show a wide range of magnetism, including room-temperature magnets,[1] spin-crossover materials,[2] single-molecule magnets (SMMs),[3] single-chain magnets (SCMs),[4] photomagnetism,[5] and magneto-optics.[6] One of the most remarkable aspects of this family, from a magnetic point of view, lies in the fact that it is possible to predict the nature of the magnetic exchange using simple orbital models, which are based on the symmetry of the magnetic orbitals.[7] However, the

* To whom correspondence should be addressed. Fax: +86-10-62751708. E-mail: gaosong@pku.edu.cn.

(1) (a) Mallah, T.; Thiébault, S.; Verdaguer, M.; Veillet, P. *Science* **1993**, *262*, 1554. (b) Ferlay, S.; Mallah, T.; Ouhaès, R.; Veillet, P.; Verdaguer, M. *Nature (London)* **1995**, *378*, 701. (c) Garde, R.; Villain, F.; Verdaguer, M. *J. Am. Chem. Soc*. **2002**, *124*, 10531. (d) Entley, W. R.; Girolami, G. S. *Science* **1995**, *268*, 397. (e) Homes, S. M.; Girolami, G. S. *J. Am. Chem. Soc*. **1999**, *121*, 5593. (f) Hatlevik, Ø.; Buschmann, W. E.; Zhang, J.; Manson, J. L.; Miller, J. S. *Adv. Mater*. **1999**, *11*, 914.

(2) (a) Niel, V.; Thompson, A. L.; Muñoz, M. C.; Galet, A.; Goeta, A. E.; Real, J. A. *Angew. Chem., Int. Ed.* **2003**, *42*, 3760. (b) Molnár, G.; Niel, V.; Gaspar, A. B.; Real, J. A.; Zwick, A.; Bousseksou, A.; McGarvey, J. J. *J. Phys. Chem. B* **2002**, *106*, 9701. (c) Molnár, G.; Niel, V.; Real, J. A.; Dubrovinsky, L.; Bousseksou, A.; McGarvey, J. J. *J. Phys. Chem. B* **2003**, *107*, 3149.

(3) (a) Sokol, J. J.; Hee, A. G.; Long, J. R. *J. Am. Chem. Soc*. **2002**, *124*, 7656. (b) Berlinguette, C. P.; Vaughn, D.; Canada-Vilalta, C.; Galán-Mascarós, J. R.; Dunbar, K. R. *Angew. Chem., Int. Ed*. **2003**, *42*, 1523. (c) Mironov, V. S.; Chibotaru, L. F.; Ceulemans, A. *J. Am. Chem. Soc*. **2003**, *125*, 9750. (d) Choi, H. J.; Sokol J. J.; Long, J. R. *Inorg. Chem*. **2004**, *43*, *1606*. (e) Schelter, E. J.; Prosvirin, A. V.; Dunbar, K. R. *J. Am. Chem. Soc*. **2004**, *126*, 15004.

(4) (a) Lescouëzec, R.; Vaissermann, J.; Ruiz-Pérez, C.; Lloret, F.; Carrasco, R.; Julve, M.; Verdaguer, M.; Dromzee, Y.; Gatteschi, D.; Wernsdorfer, W. *Angew. Chem., Int. Ed*. **2003**, *42*, 1483. (b) Toma, L. M.; Lescouëzec, R.; Lloret, F.; Julve, M.; Vaissermann, J.; Verdaguer, M. *Chem. Commun*. **2003**, 1850. (c) Wang, S.; Zuo, J. L.; Gao, S.; Song, Y.; Zhou, H. C.; Zhang, Y. Z.; You, X. Z. *J. Am. Chem. Soc*. **2004**, *126*, 8900.

10.1021/ic701387z CCC: $37.00
Published on Web 10/23/2007

magneto−structural correlation still remains somewhat unclear because the discrete polynuclear molecules and suitable cyanide-bridged chain compounds that can provide genuine examples for easy and deep study are not easily obtained by a so-called "brick and mortar" method in which $[M(CN)_6]^{n-}$ block serves as the brick and the naked metal ion or unsaturated coordinated complex $[M'(L)]^{m+}$ serves as the mortar, often affording the highly insoluble three-dimensional Prussian blue analogues.

An alternative strategy, which is used by several research groups,[8−11] is to decrease the number of cyanide ligands of the hexacyanometalate $[M(CN)_6]^{n-}$ precursor by blocking some of its coordination sites with chelating ligands. This strategy provides better control of the dimensionality of the final outcome when carefully selecting the building blocks of both the negative charged $[M(L)(CN)_x]^{n-}$ and the positive charged $[M'(L')]^{m+}$. Nowadays, series of bimetallic assemblies in this new family with interesting magnetic properties have been reported, for example. (1) 0D, including high-nuclearity metal−cyanide cages and high-spin trinuclear, tetranuclear, and heptanuclear complexes.[8−9] Diamagnetic Co^{III} and Ni^{II} coordinated in a square-planar geometry were introduced in building some cubic structures,[8a−d] which are not very interesting from a magnetic point of view. However, what is notable is that some complexes based on tricyanometalate precursors[13] exhibit some features of SMM, such as frequency-dependent out of phase signals in their ac susceptibility, but further evidence should be sought in the measurement at temperatures below 1.8 K. (2) 1D, including several kinds unusual chains: crossed triple chains[8d] $\{Mn[Cr(Me_3tacn)(CN)_3]_3\}_n$ (tacn = 1,4,7-triazacyclononane), the bimetallic crossed double chains[4a,10−11] $[M^{III}(L)(CN)_4]_2M'^{II}(H_2O)_2\}\cdot 4H_2O$ [M = Fe; M′ = Mn, Co, and Zn, with L = 1,10-phenanthroline (phen), 2,2′-bipyridine (bpy); M = Cr, M′ = Mn, with L = phen] in which the cobalt compounds show SCM-like properties, the bis double-zigzag chains $\{[Fe^{III}(bpy)(CN)_4]2M^{II}(H_2O)\}\cdot MeCN\cdot 0.5H_2O$ (M = Zn, Mn, and Co) exhibiting metamagnetism with T_C = 7 K and H_C = 600 Oe, ladder-like chains, and a branched zigzag chain[4b,9c,10b] $[Fe^{III}(bpca)(CN)_3Mn^{II}(H_2O)_3][Fe^{III}(bpca)(CN)_3]\cdot 3H_2O$ [bpca = bis(2-pyridylcarbonyl)amidate] exhibiting a ferromagnetic ordering below 2.0 K. (3) 2D, a novel two-dimensional compound, which is the first mixed cyano/azido-bridged coordination polymer exhibiting metamagnetism with T_C = 21 K and H_C = 5 kOe at 1.8 K, which was report in our previous communication.[11]

Our previous results demonstrate that it is possible to use a neutral or charged secondary or even third coligand, such as 2,2′-bpy, 4,4′-bpy, N_3^-, $N(CN)_2^-$, or $C_2O_4^{2-}$, together with cyanide ligands to adjust the structures.[11] Tetradentate salen-type Schiff base is a type of popular ligand which often serves as a co-ligand in building coordinating polymers. Some results have been reported in which Mn^{III}−Schiff bases act as the precursors in cyanide-bridged complexes. Mn^{III} possesses strong uniaxial anisotropy induced by the Jahn−Teller distortion of its Mn^{III} metal ions in an octahedral ligand field. Thus, a family of complexes $[\{Mn^{III}(R\text{-salen})(S)\}_n\{M^{III}(CN)_6\}]^{-(3-n)}$ (R-salen = salen-type Schiff-base ligand; S = a terminal ligand such as H_2O or alcohols; M^{III} = Fe, Cr) has been synthesized so far, but very few compounds have been structurally characterized: with n = 1, $(NEt_4)_2[Mn(saldmen)(H_2O)][Fe(CN)_6]$ ($saldmen^{2-}$ = *N*,*N*-(1,1-dimethylethylene)bis(salicylideneiminato)dianion);[12a] with n = 2, $K[Mn(5\text{-}Rsalen)]_2[M(CN)_6]$ (M = Fe, Cr)[12b−d] and $(NEt_4)[Mn(salmen)(EtOH)]_2[Fe(CN)_6]$ ($salmen^{2-}$ = *N*,*N*-(1-methylethylene)bis(salicylideneiminato) dianion);[12a] and with n = 6, $\{[Mn\text{-}(salen)(H_2O)]_6[M(CN)_6]\}\{M(CN)_6\}$ (M = Fe, Cr) ($salen^{2-}$ = *N*,*N*-ethylenebis(salicylideneiminato)-dianion).[12e−g] What is notable and interesting, among these complexes is that those with n = 2 or 3 possess SMM behavior.[12c,d,h] Here we present five new chain complexes obtained by assembly of $[Cr^{III}(L)(CN)]^-$ and $[Mn^{III}(salpn)]^+$ building blocks (L = 2,2′-bipy or 9,10-phen; salpn = a series of tetradentate Schiff base ligands based on substituted salicyldehyde, Scheme 1) where the Mn^{III} ion is well blocked in its equatorial positions by the Schiff-base ligands.

(5) (a) Sato, O.; Iyoda, T.; Fujishima, A.; Hashimoto, K. *Science* **1996**, *272*, 704. (b) Sato, O.; Einaga, Y.; Iyoda, T.; Fujishima, A.; Hashimoto, K. *Inorg. Chem.* **1999**, *38*, 4405. (c) Shimamoto, N.; Ohkoshi, S.; Sato, O.; Hashimoto, K. *Inorg. Chem.* **2002**, *41*, 678. (d) Yokoyama, T.; Okamoto, K.; Ohta, T.; Ohkoshi, S.; Hashimoto, K. *Phys. Rev. B* **2002**, *65*, 064438. (e) Sato, O. *Acc. Chem. Res.* **2003**, *36*, 692 and references therein.

(6) (a) Mizuno, M.; Ohkoshi, S.; Hashimoto, K. *Adv. Mater.* **2000**, *12*, 1855. (b) Ohkoshi, S.; Mizuno, M.; Hung, G.; Hashimoto, K. *J. Phys. Chem. B* **2000**, *104*, 8365.

(7) Kahn, O. *Molecular Magnetism*; VCH: New York, 1993.

(8) (a) Heinrich, J. L.; Berseth, P. A.; Long, J. R. *Chem. Commun.* **1998**, 1231. (b) Berseth, P. A.; Sokol, J. J.; Shores, M. P.; Heinrich, J. L.; Long, J. R. *J. Am. Chem. Soc.* **2000**, *122*, 9655. (c) Sokol, J. J.; Shores, M. P.; Long, J. R. *Angew. Chem., Int. Ed.* **2001**, *40*, 236. (d) Sokol, J. J.; Shores, M. P.; Long, J. R. *Inorg. Chem.* **2002**, *41*, 3052. (e) Heinrich, J. L.; Sokol, J. J.; Hee, A. G.; Long, J. R. *J. Solid State Chem.* **2001**, *159*, 293.

(9) (a) Oshio, H.; Tamada, O.; Onodera, H.; Ito, T.; Ikoma, T.; Tero-Kubota, S. *Inorg. Chem.* **1999**, *38*, 5686. (b) Oshio, H.; Yamamoto, M.; Ito, T. *Inorg. Chem.* **2002**, *41*, 5817. (c) Lescouëzec, R.; Lloret, F.; Julve, M.; Vaissermann, J.; Verdaguer, M. *Inorg. Chem.* **2002**, *41*, 818. (d) Lescouëzec, R.; Vaissermann, J.; Lloret, F.; Julve, M.; Verdaguer, M. *Inorg. Chem.* **2002**, *41*, 5943. (e) Karadas, F.; Schelter, E. J.; Prosvirin, A. V.; Bacsa, J.; Dunbar, K. R. *Chem. Commun.* **2005**, 1414.

(10) (a) Černák, J.; Orendáč, M.; Potočňák, I.; Chomič, J.; Orendáčová, A.; Skoršepa, J.; Feher, A. *Coord. Chem. Rev.* **2002**, *224*, 51. (b) Zhang, Y. Z.; Gao, S.; Wang, Z. M.; Su, G.; Sun, H. L.; Pan, F. *Inorg. Chem.* **2005**, *44*, 4534.

(11) (a) Lescouëzec, R.; Lloret, F.; Julve, M.; Vaissermann, J.; Verdaguer, M.; Llusar, R.; Uriel, S. *Inorg. Chem.* **2001**, *40*, 2065. (b) Toma, L.; Lescouëzec, R.; Vaissermann, J.; Delgado, F. S.; Ruiz-Pérez, C.; Carrasco, R.; Cano, J.; Lloret, F.; Julve, M. *Chem.-Eur. J.* **2004**, *10*, 6130. (c) Zhang, Y. Z.; Gao, S.; Sun, H. L.; Su, G.; Wang Z. M.; Zhang, S. W. *Chem. Commun.* **2004**, 1906.

(12) (a) Miyasaka, H.; Ieda, H.; Matsumoto, N.; Re, N.; Crescenzi, R.; Floriani, C. *Inorg. Chem.* **1998**, *37*, 255. (b) Miyasaka, H.; Matsumoto, N.; Okawa, H.; Re, N.; Gallo, E.; Floriani, C. *J. Am. Chem. Soc.* **1996**, *118*, 981. (c)Choi, H. J.; Sokol, J. J.; Long, J. R. *Inorg. Chem.* **2004**, *43*, 1606. (d) Miyasaka, H.; Takahashi, H.; Madanbashi, T.; Sugiura, K.; Clérac, R.; Nojiri, H. *Inorg. Chem.* **2005**, *44*, 5969. (e) Shen, X.; Li, B.; Zou, J.; Hu, H.; Xu, Z. *J. Mol. Struct.* **2003**, *657*, 325. (f) Shen, X.; Li, B.; Zou, J.; Xu, Z.; Yu, Y.; Liu, S. *Trans. Met. Chem.* **2002**, *27*, 372. (g) Choi, H. J.; Sokol, J. J.; Long, J. R. *J. Phys. Chem. Solids* **2004**, *65*, 839. (h) Ferbinteanu, M.; Miyasaka, H.; Wernsdorfer, W.; Nakata, K.; Sugiura, K.; Yamashita, M.; Coulon, C.; Clérac, R. *J. Am. Chem. Soc.* **2005**, *127*, 3090.

(13) (a) Wang, S.; Zuo, J. L.; Zhou, H. C; Choi, H. J.; Ke, Y. X.; Long, J. R.; You, X. Z. *Angew. Chem., Int. Ed.* **2004**, *43*, 5940. (b) Schelter, E. J.; Prosvirin, A. V.; Dunbar, K. R. *J. Am. Chem. Soc.* **2004**, *126*, 15004. (c) Li, D. F.; Parkin, S.; Wang, G. B.; Yee, G. T.; Prosvirin, A. V.; Holmes, S. M. *Inorg. Chem.* **2005**, *44*, 4903.

Scheme 1. Schiff Base Ligands (salpn) Used in This Study

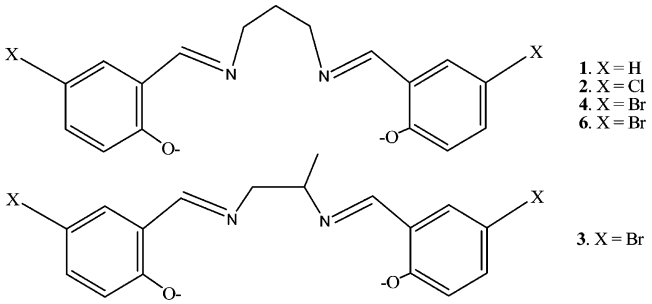

Magnetic studies show that these compounds all exhibit a transition from antiferromagnet to a ferrimagnetic state, which is found to be ruled by the feature of their structures.

Experimental Section

Preparation. All staring materials were commercially available, reagent grade, and used as purchased. Elementary analyses of C, H, and N were carried out on an Elementary Vario EL analyzer.

The precursors of $[N(CH_3)_4][Cr(bpy)(CN)_4]\cdot 5H_2O$ and $[Cr(phen)_2(CN)_2][Cr(phen)(CN)_4]\cdot 2H_2O$ were prepared by the reported methods.[11b,14] The Schiff-base ligands were prepared by condensation of a substituted salicylic aldehyde and a diamine in ethanol solution with high yields.[15] The $[Mn^{III}(salpn)]ClO_4$ precursors were prepared as follows. A yellow solution of Schiff base in methanol was mixed with equal molar amount of $Mn^{III}(OAc)_3$ and twice the amount of $NaClO_4$. The mixture was stirred for several hours; then most of the solvent was evaporated using a rotating evaporator. The dark brown solid products were purified by recrystallization in methanol/water (v/v 1:1) with the yields of ca. 40%.[16]

Crystal samples of compounds **1**−**5** were prepared by slow evaporation of solutions dissolved in equal molar amounts of $[CrL(CN)_4]$ and [Mn(salpn)] precursors. Typical for **1**: $[N(CH_3)_4][Cr(bpy)(CN)_4]\cdot 5H_2O$ (42 mg, 0.10 mmol) and $[Mn(1,3\text{-salpn})]ClO_4$ (43 mg, 0.10 mmol) were dissolved in methanol (20 mL), and the mixture was stirred for 2 h and then filtrated, and the resulting solution was left to allow slow evaporation. Dark brown crystals of **1** were obtained after 2 weeks. Yield: 32 mg, 45%. Using $[N(CH_3)_4][Cr(bpy)(CN)_4]\cdot 5H_2O$ and other $[Mn(salpn)]ClO_4$ precursors crystalline products of compounds of **2**, **3**, and **4** were obtained in yields of 39%, 26%, and 23%. Compound **5** was prepared using $[Cr(phen)_2(CN)_2][Cr(phen)(CN)_4]\cdot 2H_2O$ and $[Mn(5Br\text{-}1,3\text{-salpn})]ClO_4$ in a yield of 27%. Anal. Calcd for **1**, $CrMnC_{33}H_{30}N_8O_4$: C, 55.86; H, 4.26; N, 15.79. Found: C, 55.75; H, 4.25; N, 16.39. IR stretching cyanide: 2156 cm^{-1}. Anal. Calcd for **2**, $CrMnC_{32}H_{28}Cl_2N_8O_4$: C, 50.15; H, 3.68; N, 14.62. Found: C, 48.63; H, 3.61; N, 14.60. IR stretching cyanide: 2140 cm^{-1}. Anal. Calcd for **3**, $CrMnC_{32}H_{28}Br_2N_8O_4$: C, 44.93; H, 3.30; N, 13.10. Found: C, 45.06; H, 3.61; N, 13.84. IR stretching cyanide: 2146 cm^{-1}. Anal. Calcd for **4**, $CrMnC_{33}H_{30}Br_2N_8O_4$: C, 45.59; H, 3.48; N, 12.89. Found: C, 43.16; H, 3.45; N, 12.78. IR stretching cyanide: 2150 cm^{-1}. Anal. Calcd for **5**, $CrMnC_{34}H_{30}Br_2N_8O_5$: C, 45.51; H, 3.39; N, 12.49. Found: C, 46.16; H, 3.21; N, 12.81. IR stretching cyanide: 2151 cm^{-1}.

X-ray Crystallography. Crystallographic data for single crystals of all compounds were collected[17a] at 293 K on a Nonius KappaCCD diffractometer with a 2.0 kW sealed tube source using graphite monochromated Mo Kα radiation of $\lambda = 0.71073$ Å. Intensities were corrected for Lorentz and polarization effects and empirical absorption.[17b] Structural calculations were performed using the SHELX program.[18] The structures were solved by direct methods and refined by full-matrix least-squares on F^2. Anisotropic thermal parameters were used for the non-hydrogen atoms. Hydrogen atoms were added geometrically and not refined.

Physical Measurements. FTIR spectra were recorded using pure samples in the range from 4000 to 650 cm^{-1} on a Nicolet Magna 750 FT/IR spectrometer. dc and ac magnetic data were obtained on a Quantum Design MPMS-5XL SQUID system. Diamagnetic corrections were estimated using Pascal constants[19] (3.19×10^{-4}, 3.44×10^{-4}, 3.84×10^{-4}, 3.91×10^{-4}, and 4.03×10^{-4} $cm^3\ mol^{-1}$ for **1**, **2**, **3**, **4**, and **5**, respectively) and background correction by experimental measurement on sample holders.

Results and Discussion

Crystal Structures. Detailed crystallographic data are summarized in Table 1, and the key bond distances and angles are listed in Table 2. Detailed molecular geometries were retrieved from the cif files. The common structural feature of these compounds is the neutral Cr−Mn bimetallic chain composed of the building blocks of $[CrL(CN)_4]^-$ and $[Mn(salpn)]^+$ alternately linked by the cyanide bridges though the chain (Figure 1). Four compounds, **1**−**4**, have very similar chain structures. As shown in Figure 1−d, in each compound the $[Cr(bpy)(CN)_4]^-$ unit connects two $[Mn(salpn)]^+$ units with the two *trans*-CN^- ligands while the two *cis*-CN^- ligands act as the end ligands. The $[Mn(salpn)]^+$ unit is axially coordinated by two $[Cr(bpy)(CN)_4]^-$ units. These Cr−C−N−Mn linkages produce the bimetallic chain of $[Cr-C-N-Mn]_n$ (2,2-TT chain[10a]) in which the two kinds of octahedral metal sites, Mn^{III} and Cr^{III}, are alternatively arranged along the chain. The chelating groups of the two building blocks are opposite, and the salpn is bent to one side. Mn^{III} shows significant Jahn−Teller distortion with short equatorial Mn−O/N (O/N from salpn) distances of 1.867−2.036 Å and longer axial Mn−N (N from CN^- bridges) distances of 2.250−2.357 Å for the four compounds, while the Cr^{III} sites have very closed Cr−C/N distances of 2.008−2.036 Å (Table 2). This is expected for Mn^{III} and Cr^{III} ions; the former is a strong Jahn−Teller ion, but the later is not.[28] It is noted that the metal−C/N/O distances show no significant change running the series. The two unique Mn−N−C angles involving bridging CN^- ligands along the chain are somewhat different as are the Cr−C−N angles (Table 2). For **1** the Mn−N−C angles in pair are 162.5°/165.5°, and Cr−C−N angles are178.1°/178.4°. For **2**−**4** the angles become smaller, viz. 147.4°/152.5° (Mn−N−C) and

(14) Mallah, T.; Auberger, C.; Vergaguer, M.; Veillet, P. *J. Chem. Soc., Chem. Commun*. **1995**, 61.
(15) Mohebi, S.; Boghaei, D. M. *Synth. React. Inorg. M-O Chem*. **2004**, *34*, 611.
(16) Przychodzen, P.; Lewinski, K.; Balanda, M.; Pelka, R.; Rams, M.; Wasiutynski, T.; Guyard-Duhayon, C.; Sieklucka, B. *Inorg. Chem*. **2004**, *43*, 2967.
(17) (a) *Collect data collection software*; Nonius B.V.: Delft, The Netherlands, 1998. (b) *HKL2000 and maXus softwares*; University of Glasgow: Scotland, U.K., Nonius B. V.: Delft, The Netherlands, and MacScience Co. Ltd.: Yokohama, Japan, 2000.
(18) Sheldrick, G. M. *SHELX-97, Program for Crystal Structure Determination*; University of Göttingen: Germany, 1997.
(19) Mulay, L. N.; Boudreaux, E. A. *Theory and Applications of Molecular Diamagnetism*; John Wiley & Sons Inc.: New York, 1976.

Table 1. Summary of Crystallographic Data for Compounds

	1	2	3	4	5
formula	$CrMnC_{33}H_{30}N_8O_4$	$CrMnC_{32}H_{28}Cl_2N_8O_4$	$CrMnC_{32}H_{28}Br_2N_8O_4$	$CrMnC_{33}H_{30}Br_2N_8O_4$	$CrMnC_{34}H_{30}Br_2N_8O_5$
M_r [g/mol]	709.59	766.46	855.38	869.41	897.42
cryst syst	monoclinic	triclinic	triclinic	triclinic	monoclinic
space	*C*2/*m*	$P\bar{1}$	$P\bar{1}$	$P\bar{1}$	$P2_1/n$
a [Å]	18.8371(4)	10.5139(8)	10.5663(6)	10.5061(4)	15.8304(4)
b [Å]	18.1726(5)	11.7534(10)	12.0949(7)	11.8547(4)	13.4057(3)
c [Å]	10.9244(3)	15.0032(13)	15.0986(10)	14.9532(7)	19.7864(6)
α [deg]	90	67.650(4)	67.683(3)	68.574(14)	90
β [deg]	121.090(2)	84.914(4)	84.657(3)	85.085(14)	112.955(10)
γ [deg]	90	88.307(3)	85.292(2)	87.627(2).	90
V [Å^3]	3202.46(14)	1708.0(2)	1775.00(19)	1727.19(12)	3866.51(18)
Z	4	2	2	2	4
ρ_{calcd} [mg/cm^3]	1.472	1.490	1.600	1.672	1.542
F(000)	1460	782	854	870	1796
cryst size [mm]	0.23 × 0.15 × 0.05	0.2 × 0.12 × 0.08	0.34 × 0.17 × 0.06	0.41 × 0.12 × 0.07	0.9 × 0.75 × 0.75
θ_{limit} [deg]	3.44−27.48	3.39−25.11	3.40−27.50	3.42−27.50	3.42−24.99
collected reflns	34 645	31 841	36 959	36 408	63 339
unique reflns	3777	6003	7526	7866	6748
R_{int}	0.1119	0.1934	0.1395	0.1588	0.1670
T_{max}/T_{min}	0.899−0.989	1.086−0.707	0.860−0.634	0.884−0.549	0.165−0.068
no. of params	3777/0/225	6003/0/433	7526/0/433	7866/0/442	6748/0/460
GOF	0.917	0.882	0.910	0.853	1.116
R1[a]	0.0422	0.0532	0.0551	0.0466	0.0636
wR2[b]	0.0953	0.1001	0.1139	0.0814	0.1568

[a] $R1 = \Sigma||F_o| - |F_c||/\Sigma|F_o|$. [b] $wR_2 = \Sigma[w(F_o^2 - F_c^2)^2]/\Sigma[w(F_o^2)^2]^{1/2}$.

Table 2. Selected Bond Lengths [Å] and Angles [deg]

	1		
Mn(1)−N_{bridge}	2.263(3)−2.305(3)	C(1)[a]−N(1)−Mn(1)	162.5(4)
Mn(1)−N(5)	2.036(2)	C(2)−N(2)−Mn(1)	165.5(4)
Mn(1)−O(1)	1.8934(19)	N(2)−C(2)−Cr(1)	178.3(4)
Cr(1)−C_{bridge}	2.079(4)−2.086(4)	N(1)[b]−C(1)−Cr(1)	177.9(4)
Cr(1)−C_{intact}	2.046(3)−2.067(3)	N(3)−C(3)−Cr(1)	178.1(3)
	2		
Mn(1)−N_{bridge}	2.261(5)−2.348(5)	C(2)−N(2)−Mn(1)	147.4(5)
Mn(1)−N/O	1.875(4)− 2.017(5)	C(1)−N(1)−Mn(1)[c]	152.5(5)
Cr(1)−C_{bridge}	2.062(7)−2.069(6)	N(1)−C(1)−Cr(1)	170.1(6)
Cr(1)−C_{intact}	2.008(6)−2.049(7)	N(2)−C(2)−Cr(1)	174.5(6)
Cr(1)−N(5)	2.063(5)	N(3)−C(3)−Cr(1)	176.8(6)
Cr(1)−N(6)	2.083(4)	N(4)−C(4)−Cr(1)	175.7(6)
	3		
Mn(1)−N_{bridge}	2.250(5)−2.357(5)	C(1)[c]−N(1)−Mn(1)	175.7(5)
Mn(1)−N/O	1.867(4)−1.988(5)	C(2)−N(2)−Mn(1)	170.5(5)
Cr(1)−C_{bridge}	2.063(6)−2.067(6)	N(1)[d]−C(1)−Cr(1)	175.7(5)
Cr(1)−C_{intact}	2.044(7)−2.051(7)	N(2)−C(2)−Cr(1)	178.5(7)
Cr(1)−N(5)	2.072(4)	N(3)−C(3)−Cr(1)	146.2(5)
Cr(1)−N(6)	2.059(5)	N(4)−C(4)−Cr(1)	155.9(5)
	4		
Mn(1)−N_{bridge}	2.260(4)−2.357(4)	C(1)[c]−N(1)−Mn(1)	146.5(3)
Mn(1)−N/O	1.877(3)−2.011(3)	C(2)−N(2)−Mn(1)	151.3(4)
Cr(1)−C_{bridge}	2.062(5)−2.068(5)	N(1)[d]−C(1)−Cr(1)	174.0(4)
Cr(1)−C_{intact}	2.049(5)−2.051(5)	N(2)−C(2)−Cr(1)	171.6(4)
Cr(1)−N(5)	2.067(4)	N(3)−C(3)−Cr(1)	175.0(4)
Cr(1)−N(6)	2.069(4)	N(4)−C(4)−Cr(1)	176.2(5)
	5		
Mn(1)−N_{bridge}	2.260(6)−2.366(6)	C(1)−N(1)−Mn(1)	147.9(5)
Mn(1)−N/O	1.873(4)−2.028(6)	C(2)[e]−N(2)−Mn(1)	161.3(6)
Cr(1)−C_{bridge}	2.060(7)−2.068(7)	N(1)−C(1)−Cr(1)	175.5(5)
Cr(1)−C_{intact}	2.061(9)−2.077(8)	N(2)[f]−C(2)−Cr(1)	176.6(6)
Cr(1)−N(5)	2.074(5)	N(3)−C(3)−Cr(1)	176.6(8)
Cr(1)−N(6)	2.066(6)	N(4)−C(4)−Cr(1)	175.5(8)

[a] *x*, *y*, *z*. [b] *x*, *y*, *z* + 1. [c] *x* + 1, *y*, *z*. [d] *x* − 1, *y*, *z*. [e] −*x* + 3/2, *y* − 1/2, −*z* + 1/2. [f] −*x* + 3/2, *y* + 1/2, −*z* + 1/2.

170.1°/174.5° (Cr−C−N), 146.2°/155.9° (Mn−N−C) and 175.7°/178.5° (Cr−C−N), and 146.5°/151.3° (Mn−N−C) and 174.0°/171.6° (Cr−C−N) for **2**, **3**, and **4**, respectively, and the smaller Mn−N−C and Cr−C−N angles result in shorter Mn···Cr distances in **2** (5.23/5.29 Å), **3** (5.27/5.30 Å), and **4** (5.23/5.28 Å) compared to that in **1** (5.45/5.47 Å). The larger deviation of the Mn−N−C and Cr−C−N angles from linearity from **1** to **4** might be due to increased stereohindrance of the salpn ligands in the compounds. For compound **5** involving a more bulky unit of $[Cr(phen)(CN)_4]^-$ compared to the $[Cr(bpy)(CN)_4]^-$ unit in **1**−**4** produced a different zigzag bimetallic 2,2-CT chain[10a] (Figure 1e) in which the $[Cr(phen)(CN)_4]^-$ unit links two $[Mn(salpn)]^+$ units with two *cis*-CN^- ligands instead of the two *trans*-CN^- ligands observed in **1**−**4**. This is probably due to this *cis*-arrangement of $[Mn(salpn)]^+$ units around the $[Cr(phen)(CN)_4]^-$ unit; the difference of the two Mn−N−C angles is large (147.9° and 162.0°). The bond distances in **5** are similar than those observed in **1**−**4** (Table 2), and the two unique intrachain Mn···Cr distances in **5** are 5.33/5.37 Å. Another interesting observation is that salpn is significantly bent toward one $[Cr(phen)(CN)_4]^-$ unit, somewhat like that in **1**, and this should be due to the packing effect in the crystal discussed as follows.

In the crystals the packing of these bimetallic chains is dominated by aromatic $\pi-\pi$ stacking interactions because of the large aromatic parts of the ligands of salpn, bipy, and

(20) Janiak, C. *J. Chem. Soc., Dalton Trans*. **2000**, *21*, 3885.
(21) (a) Dance, I.; Scudder, M. *J. Chem. Soc., Dalton Trans*. **2000**, *10*, 1587. (b) Russell, V.; Scudder, M.; Dance, I. *J. Chem. Soc., Dalton Trans*. **2001**, *6*, 789.
(22) Shu, C.; Leitner, A.; Hartwing, J. F. *Angew. Chem., Int. Ed*. **2004**, *43*, 2798.
(23) Choi, H. J.; Sokol, J. J.; Long, J. R. *J. Phys. Chem. Solids* **2004**, *65*, 39−844.
(24) Rebilly, J. N.; Mallah, T. *Single Molecule Magnets and Related Phenomena*; Springers-Verlag: Berlin Heidelberg, 2006.
(25) Pei, Y.; Kahn, O.; Sletten, J.; Renard, J. P.; Georges, R.; Gianduzzo, J. C.; Curely, J.; Xu, Q. *Inorg. Chem.* **1988**, *27*, 47.
(26) Ferlay, S.; Mallah, T.; Ouahès, R.; Veillet, P.; Verdaguer, M. *Inorg. Chem*. **1999**, *38*, 229.
(27) Ohkoshi, S.; Hashimoto, K. *Chem. Phys. Lett*. **1999**, *314*, 210.
(28) Caneschi, A.; Gatteschi, D.; Sessoli, R.; Barra, A. L.; Brunel, L. C.; Guillot, M. *J. Am. Chem. Soc*. **1991**, *113*, 5873.

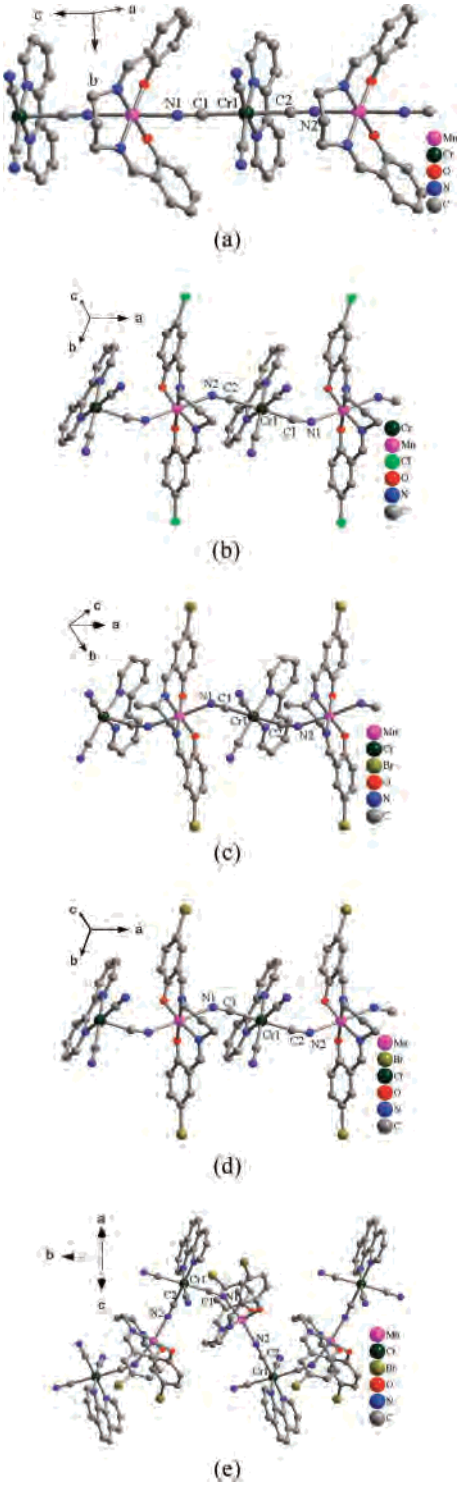

Figure 1. Chain structures in ball−stick model of compounds **1**−**5** (a−e), respectively.

phen (Supporting Information Figures S1−S3). For compound **1** the chains are running along the *c* direction, and the chains form layers parallel to the *bc* plane. In the layer each chain interacts with two other adjacent chains via face-to-face $\pi-\pi$ stacking between the benzene rings of the salpn ligand of the $[Mn(salpn)]^+$ units (Supporting Information Figure S1a). The plane-to-plane distance is 3.61 Å, and the offset angle[20] is 35°. The adjacent chains are also held together by the weak H bonds between the terminal cyanides of $[Cr(bpy)(CN)_4]^-$ units in one chain and the C−H donors of bipy ligands in neighboring chains. The 3D structure is the layers stacking along *a* direction mainly via van der Waals interaction with disordered solvent water and methanol filling the interstices between the layers. (Figure S1b), though some H-bonding interactions between the solvents and the terminal cyanide ligands are possible. In the nearest layer the interchain metal−metal separation is 9.10 Å, while the nearest interlayer separation is 8.04 Å.

Compounds **2**−**4** have a very similar packing pattern of the chain in their crystals; therefore, **2** is representative here for discussion (Figure S2). The crystal structure can be considered as a nearly hexagonal arrangement (Figure S2b) of the double chain (Figure S2a) in which two bimetallic chains interact via face-to-face $\pi-\pi$ stacking among the bipy ligands as well as chlorobenzene rings of salpn. The geometries have a plane-to-plane distance of 3.47 Å and offset angle of 23° for bipy to bipy overlaps and 3.56 Å and 40° for chlorobenzene to chlorobenzene rings of salpn. It is of merit to point out that the bipy's are in the interior of the doubled chain while the salpn's are outside. The more significant $\pi-\pi$ stacking results in a short metal−metal distance of 7.64 Å between the two chains in the double chain. In the hexagonal stacking of the doubled chain it is noted that in *b*−*c* direction one set of chlorobenzenes of the adjacent double chains are face-to-face overlapped in pair with the Cl atom of one chlorobenzene nearly over the benzene ring center of other chlorobenzene and vise versa. The interstices between the double chains are occupied by solvent water and methanol. With very similar crystal structures, compounds **3** and **4** possess very similar interchain interactions and geometries compared to **2**.

Finally, the different zigzag chain of compound **5** resulted in a very different packing pattern (Figure S3). In the crystal the zigzag chain runs along the *b* direction, and they are arranged parallel along the *ab* plane to form a condensed layer (Figure S3a). The interactions in the layer might be Br···N and C−H···N type[29] between the adjacent chains in which N is the N end of the terminal cyanide ligands. The phen and one of the bromobenzene rings of salpn are on the two sides of the layer. When these layers stack along the *c* direction with two adjacent ones centrosymmetrically related, both phen and the bromobenzene ring are involved in significant aromatic interactions. The two phen's from adjacent layers form a face-to-face $\pi-\pi$ stacking, and this phen dimer is further embraced by two bent salpn ligands, resulting in edge-to-face interaction from phen to the bromobenzene ring of salpn. This pattern is so-called P4AE aryl embrace.[21] This P4AE aryl embrace pattern extends along the *a* direction, and between them the bromobenzene rings form another aryl interaction, the OFF type. Therefore, 1D P4AE-OFF-P4AE-OFF aryl embrace patterns are observed in between the layers (Figure S3b). It is interesting to see that the whole 3D structure is porous with channels along the *a* direction, and the channel is ca. 3 × 5 Å wide

(29) (a) Steiner, T. *Angew. Chem., Int. Ed.* **2002**, *41*, 48. (b) Desiraju, G. R.; Steiner, T. *The Weak Hydrogen Bond In Structural Chemistry and Biology*; Oxford University Press: New York, 1999.

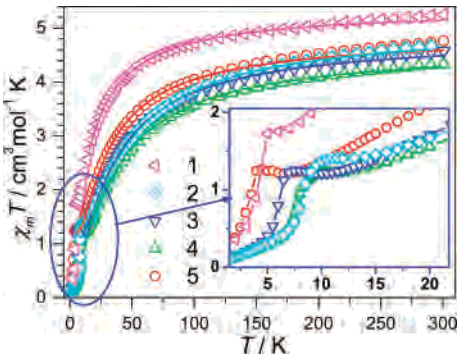

Figure 2. Temperature dependence of magnetic susceptibility (per CrMn, under field of 1 kOe) for compounds **1**−**5**. Solid lines are best fits by the alternating chain model (see text). (Inset) Low-temperature region.

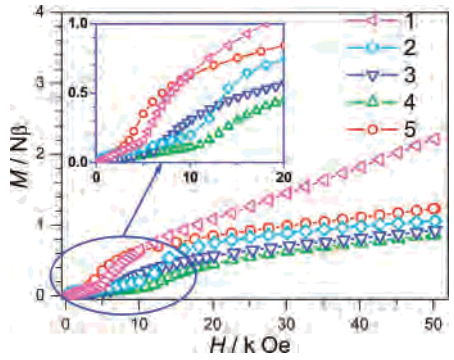

Figure 3. Field-dependent magnetizations at 1.9 K for **1**−**5**.

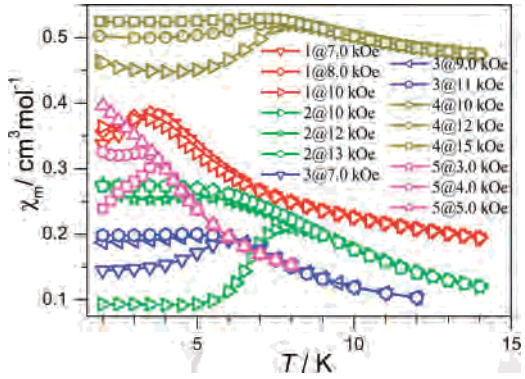

Figure 4. FC measurement at different fields.

and occupied by solvents of water and methanol (Figure S3c). Porous structures made by chain-like motifs are still rare,[22] and this compound might be of interest for further study on its porosity. Due to more bulky ligands, the separation of the nearest interchain metal is as far as 9.19 Å in **5**.

Magnetic Properties.

The structures of these series feature cyanide-bridged bimetallic chains of $[Cr-C-N-Mn]_n$ further stacking through $\pi-\pi$ interactions and weak H bonds, thus possessing strong intrachain couplings with weak interchain couplings. It is expected that these compounds should exhibit low-dimensional magnetism. Indeed, magnetic investigation revealed that the compounds are all metamagnets (Figures 2−4 and Supporting Information Figures S4−S6) with differences in details (Table 3). The temperature dependence of their susceptibilities under a 1 kOe applied field is shown in Figure 2. The experimental $\chi_m T$ values per $Cr^{III}Mn^{III}$ at

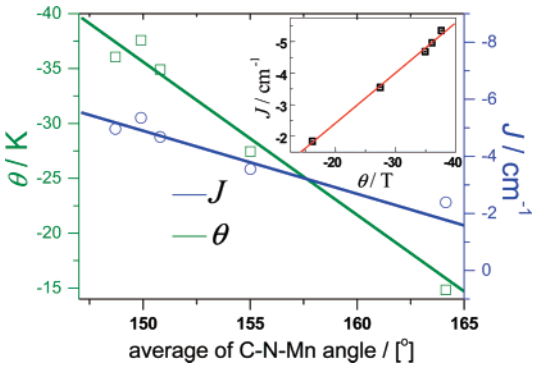

Figure 5. Correlation between some magnetic properties and structures: the intrachain couplings (J), Weiss temperatures (θ), and Mn−N−C angles (α).

300 K are 4.33−5.03 cm^3 mol^{-1} K (Table 3), and these are expected for one uncoupled Cr^{III} and one Mn^{III} (4.88 for the sum of one spin-only Cr^{III}, $S = 3/2$, and one Mn^{III}, $S = 2$, with $g = 2.00$) though a slightly higher value is observed for **1**. Upon cooling the $\chi_m T$ values decrease gradually and reach a short plateau around 10 K ($\chi_m T$ values 1.20−1.72 cm^3 mol^{-1} K, Table 3) then go down more quickly to be close to zero. For all compounds the high-temperature data obey the Curie−Weiss law (Figure S5), giving Weiss temperatures from −14.8 to −37.6 K and the Curie constants from 4.84 to 5.29 cm^3 mol^{-1} K (Table 3). The negative Weiss temperature values indicate dominant antiferrimagnetic (AF) coupling in all materials. Considering the structures it is rational that the intrachain couplings, i.e., those between the Cr^{III} and Mn^{III} ions, are AF type, as observed in other cyanide-bridged Cr/Mn compounds.[3d,23] As the Cr^{III} and Mn^{III} ions possess uncompensated spins, these intrachain AF couplings, in fact, produce ferrimagnetic (FI) chains. In $\chi_m T$ vs T plot the $\chi_m T$ value decreases gradually following the decreasing temperature, and there is a short plateau area around 10 K, suggesting the ferrimagnetic state competing with the interchain AF coupling, and a further quick decrease of $\chi_m T$ after the plateau should be due to the 3D AF ordering by the AF interactions between the ferrimagnetic chains.

The metamagnetic behaviors of these materials are further characterized by the field-dependent magnetizations at 1.9 K, showing pronounced sigmoid behavior (Figure 3). The magnetizations first increase slowly as the field increases because of the AF interchain interactions and then transit to a FI state at critical fields of several to tens kOe (Table 3, estimated by peaks of dM/dH vs H); after that, they increase nearly linearly and slowly with the field. At 50 kOe the magnetization values reach ca. 1 Nβ for **2**−**5** (Table 3), corresponding to the expected ferrimagnetic state $S_T = 4/2-3/2 = 1/2$ per CrMn unit. For **1** the magnetization at 50 kOe is 2.2 Nβ; this might be due to related weak intrachain AF coupling (see later and Figure S8) in **1**, where the antiparallely aligned spins are gradually aligned by high fields. The lower critical fields observed for **1** and **5** contribute to the larger interchain metal−metal separations and thus weak interchain couplings in the materials compared to compounds **2**−**4**. In addition, **1** displays a small hysteresis with coercive field of 400 Oe (Figure S4); this might indicate that the

Table 3. Collection for Magnetic Results of Compounds **1**−**5**

	Curie−Weiss Fit		alternating chain mod el fit								$\chi_m T$ cm^3 m ol^{-1} K		
	C, cm^3 mol^{-1} K	θ, K	J, cm^{-1}	α, cm^{-1}	ZJ, cm^{-1}	g_{Mn}	g_{Cr}	T_N, K	H_c, kOe	Ms, Nβ	2.0 K	300 K	plat.
1	5.29	−14.83	−2.39	0.012	−0.25	2.10	1.89	4.4	6.03	2.22	0.35	5.03	1.72
2	5.26	−37.57	−5.35	−2.5E^{-5}	−0.53	2.02	2.08	8.1	12.1	1.06	0.13	4.67	1.40
3	5.10	−34.90	−4.68	−0.40	−0.45	1.90	2.14	6.0	8.17	0.92	0.15	4.58	1.25
4	4.84	−36.06	−4.96	0.17	−0.64	1.89	2.08	7.8	13.1	0.86	0.12	4.33	1.20
5	5.16	−27.44	−3.55	−0.15	−0.38	1.96	2.08	3.7	4.02	1.23	0.38	4.76	1.26

Scheme 2 Alternating Ferrimagnetic Chain Model[25] Used for Evaluating the Intrachain Coupling

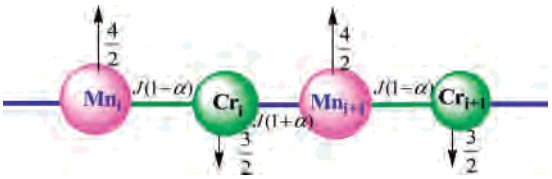

noncollinear character of the AF interaction between FI chains in the material; compounds **1**−**4** display thin butterfly-like hysteresis after the AF-FI transition (Figure S4).

Furthermore, field-cooled magnetizations (FC) under different fields were investigated and are shown in Figure 4. For all compounds in low fields the χ_m vs T curves all display a maximum, suggesting the occurrence of 3D AF ordering in these materials. Upon increasing field the maximum moved to lower temperatures, became less prominent, and finally disappeared (or almost disappeared) above the critical fields, confirming the metamagnetic transitions. All compounds show no frequency-dependent ac susceptibilities under zero dc field (Figure S5), and the out of phase responses (χ'') are almost undetectable, as expected for antiferromagnets, and the Néel temperatures (T_N) for the global AF transition, estimated from the positions of the peaks of d($\chi' T$)/dT at 100 Hz, listed in Table 3, are between ranging from 3.7 to 8.1 K.

Therefore, these materials are all metamagnets showing AF to FI transitions due to strong intrachain uncompensated AF coupling and weak interchain AF coupling. Because the chains possess two kinds of CN^- bridges with different bond geometries the two unique couplings along the chain should be of different magnitudes. In these cases a regular chain model is not proper for evaluating the intrachain couplings. An alternative chain model (Scheme 2) was used.[25] The spin Hamiltonian is $H = -J\Sigma_i S_{Cri}\cdot[(1+\alpha)S_{Mni}+(1-\alpha)S_{Mni+1}]$, where the local spins are S_{Cr} and S_{Mn}, the local Zeeman factors g_{Cr} and g_{Mn}, and the couplings between nearest neighbors $J(1+\alpha)$ and $J(1-\alpha)$. The best fit of the magnetic data above T_N, including a molecular field approach for the interchain magnetic interaction (zJ'), gave the parameters summarized in Table 3 with agreeable factors of $R = 10^{-5}$−10^{-6}, $\{R = \Sigma[\chi_{m,obs} - \chi_{m,calcd}]^2/\Sigma\chi_{m,obs}^2\}$.[7] Note that the intrachain coupling of **1** is significantly smaller than that of other compounds, and this should be the reason for the somewhat different behavior of **1** in field-dependent magnetizations compared to other compounds (Figure 3); further discussion is given in the Supporting Information, Figure S8. The negative zJ's confirmed interchain AF interactions, resulting in the dominant antiferromagnetic ground state in all these materials, and these interchain AF interactions are overcome by higher fields to turn the materials into ferrimagnetic states. It was found that H_C, zJ', T_N, and the shortest interchain metal−metal separations are closely correlated: higher transition fields, stronger interchain AF interactions as well as higher T_N in accorded with compact alignment of the chains, which was studied from the shortest interchain metal−metal separations very qualitatively (Figure S7).

The recent studies and analyses for a number of compounds with M′−N−C−M linkages have developed some rules for the role of the cyanide bridge in magnetic exchange between metal sites: (1) the cyanide bridge can transmit ferromagnetic (FO) and AF interactions between transition-metal ions depending on the symmetry of the magnetic orbitals;[7] (2) the direct exchange interactions between transition-metal ions are almost zero;[24] (3) the critical temperature T_C follows[26] $T_C = (2/k_B)y^{3/2}[S_M(S_M+1)S_{M'}(S_{M'}+1)]^{1/2}$ (y is the stoichiometry); and (4) $J_{MM'}$ can be estimated by[27] $J_{MM'} = (1/mn)\Sigma_{i=1}{}^m\Sigma_{j=1}{}^n J_{ij}$. Obviously, the details such as the deviation of M′−N−C−M linkage from linearity have been ignored for simplicity. In our previous report[10b] we revealed that for several Cr^{III}−N−C−Mn^{II} compounds based on $[Cr(bpy)(CN)_4]^-$ blocks the larger AF coupling corresponds to the higher bending of the Cr−C−N−Mn unit, and this has been confirmed recently by Julve and co-worker.[11b] The magnetic couplings (J) between −4.7 and −9.4 cm^{-1}, which, together with those Julve's reported,[11b] show a linear relationship with the Mn−N−C angle (α, deg): J (cm^{-1}) = $-40 + 0.2\alpha$. When the angle deviates from a collinear arrangement (180°), the overlap of two coupling orbitals probably increases, and consequently, an increase in J_{AF} will follow. The same approach can be applied to analyze the Cr^{III}−Mn^{III} compounds in this work. We plotted the data J and θ (Weiss temperature) vs the average angle of Mn−N−C (Figure 5); it exhibits a similar linear relationships with J (cm^{-1}) = $-33 + 0.18\alpha$ and θ (K) = $-257.9 + 1.5\alpha$. In $Cr^{III}(t_{2g}{}^3e_g{}^0)$−$Mn^{II}(t_{2g}{}^3e_g{}^2)$ there are six ferromagnetic exchanging approaches via electrons in the orthogonal t_{2g}(Cr) and e_g(Mn) orbitals, and the t_{2g}−t_{2g} pathway is ensured to transfer AF coupling. In the situation of Cr^{III}−Mn^{III} here there are only one-half the ferromagnetic approaches as the Cr^{III}−Mn^{II} pair has because there is only one electron in the e_g orbitals of Mn^{III}. However, a similar linear relationship is obtained with very similar parameters of slope and intercept of the line.

Conclusion

In this work, we synthesized five one-dimensional Cr^{III}−Mn^{III} alternating chains by assembly of $[Mn^{III}(salpn)]^+$ and $[Cr^{III}(bipy)(CN)]^-$ (compounds **1**−**4**) or $[Cr^{III}(phen)(CN)]^-$ building blocks (compound **5**). The bimetallic chains of the

four compounds **1**−**4** are straight as the [Cr(bpy)$(CN)_4$] unit, with its two *trans*-cyanide ligands, connects the two neighboring [Mn(salpn)] units at axial positions, while in **5** the chain is zigzag because the [Cr(phen)$(CN)_4$] unit connects the [Mn(salpn)] units with its two *cis*-cyanide ligands. The chains are stacking via weak interactions, mainly the aromatic $\pi-\pi$ type. The compounds are all metamagnets showing AF to FI transition due to weak interchain AF interactions between the FI bimetallic chains. The intrachain AF couplings, between cyanide-bridges Cr^{III} and Mn^{III} ions, were estimated to be from -1.84 to -5.35 cm^{-1} in the materials and follow a linear relationship to the Mn−N−C angles, similar to cyanide-bridges Cr^{III} and Mn^{II} systems. The weak interchain AF interactions and the fields for the AF−FI transition are closely related to the separations between FI chains in the materials. Finally, the synthetic approach will be useful to explore bimetallic systems with other 3d metals such as Co^{II}, Cu^{II}, and Ni^{II}, which have more electrons in the e_g magnetic orbital, as substitutions of Mn^{III}, and this may bring about a deeper understanding of the magnetic interaction in cyanide-based magnetic materials.

Acknowledgment. This work was supported by the National Natural Science Foundation of China (grants 20221101, 20490210, and 20571005), the National Basic Research Program of China (grant 2006CB601102), and the Research Fund for the Doctoral Program of Higher Education (grant 20050001002).

Supporting Information Available: CIF files of **1**−**5**, a pdf file containing Figures S1−S6. This material is available free of charge via the Internet at http://pubs.acs.org.

IC701387Z